Synergistic Effects of Side-Chain Engineering and Fluorination on Small Molecule Acceptors to Simultaneously Broaden Spectral Response and Minimize Voltage Loss for 13.8% Efficiency Organic Solar Cells

Qunping Fan, Wenyan Su, Ming Zhang, Jingnan Wu, Yufeng Jiang, Xia Guo, Feng Liu, Thomas P. Russell, Maojie Zhang, and Yongfang Li*

Herein, three small molecule (SM)-acceptors (POIT-IC, POIT-IC2F, and POIT-IC4F) are developed by combining the side-chain engineering located on the sp^3-hybridized carbon atoms of the fused-ring core and the fluorination of end groups. From ITIC to POIT-IC, POIT-IC2F, and then to POIT-IC4F, the SM- acceptors show gradually broadened absorption spectra, increased maximum extinction coefficient, crystallinity, and electron mobilities due to the synergistic effects of side-chain engineering and fluorination. Compared with nonfluorinated ITIC and POIT-IC, as fluorination broadens the molecular spectra, POIT-IC2F and POIT-IC4F with alkoxyphenyl side chains show less decreased LUMO levels than IT-IC2F and IT-IC4F with alkylphenyl side chains, which are conducive to both higher V_{oc} and J_{sc} for organic solar cells (OSCs). Combined with polymer donor PM6, the POIT-IC4F-based OSCs achieve a device efficiency of up to 13.8% with a high V_{oc} of 0.91 V and J_{sc} of 20.9 mA cm^{-2}, which are significantly higher than that of the control OSCs based on ITIC (8.9%), POIT-IC (10.1%), or IT-IC4F (12.2%). An efficiency of 13.8% is one of the highest PCEs reported for the annealing-free OSCs. Our results show that the synergistic effects of side-chain engineering and fluorination on SM-acceptor can simultaneously broaden spectral response and minimize voltage loss of OSCs and ultimately achieve high device efficiency.

1. Introduction

In the last three decades, organic solar cells (OSCs) based on ful- lerene derivative acceptors have been enormously investigated because of their potential applications in roll-to-roll and translucent solar panels,[1] and have achieved power conversion effi- ciencies (PCEs) over 11%.[2–4] However, some inherent disadvantages, such as weak absorption coefficient in UV–Vis region, and poor morphological stability restrict the further promotion of device perfor- mance. To overcome the drawbacks of ful- lerene acceptors, plenty of nonfullerene (NF) acceptors which possess the advan- tages of easy adjusting absorption and elec- tronic energy levels have been developed since 2015.[5–20] Among the NF-acceptors, the acceptor–donor–acceptor (A-D-A)-type small molecule (SM)-acceptors with adjust- able molecular energy levels, strong photo capture capability, and high carrier mobil- ity, especially ITIC[21] derivatives (such as *m*-ITIC,[22] IT-IC4F,[23] and Y6[24]), are extensively concerned. Also the single-junction OSCs based on such SM-acceptors have obtained PCEs up to 13% 16%.[25–38] The rapid development of ITIC deriva- tives has benefited mainly from their easily modified modular skeleton that consist of three components: large fused-ring electron-donating core, four non-conjugated bulk alkyl side chains, and two strong electron-accepting end groups.[39–42] Therefore, to develop efficient SM-acceptors, the

Dr. Q. Fan, Dr. W. Su, J. Wu, Prof. X. Guo, Prof. M. Zhang, Prof. Y. Li Laboratory of Advanced Optoelectronic Materials College of Chemistry, Chemical Engineering and Materials Science Soochow University
Suzhou 215123, China
E-mail: mjzhang@suda.edu.cn

Prof. M. Zhang, Prof. F. Liu
Department of Physics and Astronomy and Collaborative Innovation Center of IFSA (CICIFSA)
Shanghai Jiaotong University
Shanghai 200240, China

Y. Jiang, Prof. T. P.
Russell Materials Sciences Division
Lawrence Berkeley National Laboratory
Berkeley, CA 94720, USA

Prof. Y. Li
Beijing National Laboratory for Molecular Sciences CAS Key Laboratory of Organic Solids
Institute of Chemistry
Chinese Academy of Sciences Beijing 100190, China

researchers have synthesized lot of high-performance ITIC deriv- atives by modifying the abovementioned three components inde-pendently. For example, by extending the conjugation system of ladder-type donor cores from five fused-ring (IDT-IC)[43] to seven fused-ring (ITIC),[21] and even twelve fused-ring (R12-4Cl),[44] ITIC derivatives achieved red-shifted absorption onsets due to the enhancement of intramolecular electron push–pull effect between donor cores and acceptor end groups. However, with the extension of π-conjugated system of fused-ring core, the cost and difficulty of molecular synthesis will increase dramatically.

Compared with the complex and difficult synthesis steps of fused-ring cores, the side-chain modification and the end-group substitution of ITIC derivatives are easier and more diverse. To improve the molecular energy levels, absorption coefficient, crys- tallinity, and intermolecular packing, researchers have developed a series of ITIC derivatives by simple side-chain engineering located on sp^3-hybridized carbon atoms in the electron-donating core.[22,27,45–47] For instance, to enhance the intermolecular pack- ing, absorption coefficient, and electron mobility, the S–S inter-actions are induced by replacing alkylphenyl of ITIC with alkylthienyl.[48] Another representative side-chain engineering that has applied into ITIC is to replace alkylphenyl groups by less bulky linear alkyl chains.[49] The resulted SM-acceptor C8-ITIC shows significantly red-shifted absorption spectrum (40 nm), higher absorption coefficient, improved crystallinity as well as more compact intermolecular packing. Moreover, the end groups of ITIC derivatives can also be easily modified by various substi- tutions with different position, number, and size, as well as electron-accepting or electron-donating abilities.[15,17,23] For example, when comparing a series of SM-acceptors with halogenated/non-halogenated end groups, the halogen atoms are conducive to broadening absorption spectra, lowering LUMO levels, increas-ing intermolecular π–π stacking, crystallinity, and thus electron mobilities.[15,50] Recently, the tetrafluoro- substituted acceptor, Y6, has achieved an impressive efficiency up to 15.7% with a high short-circuit current density (J_{sc}) of 25.2 mA cm ^{2} and a high fill factor (FF) of 76.1%.[24] However, almost all strategies to broaden the absorption spectra of SM-acceptors result in a seriously decreased LUMO levels. Ultimately, the related OSCs will achieve a significantly reduced V_{oc}, which means that it is difficult to broaden the absorption spectra of SM-acceptors while minimizing the voltage loss of the related OSCs.

In this study, we developed a series of new SM-acceptors (POIT-IC, POIT-IC2F, and POIT-IC4F) by combining the alkoxy side-chain engineering located on sp^3-hybridized carbon atoms of fused-ring core and the fluorination of end groups as shown in Scheme 1, and systematically studied their effects on the photo- electronic properties of the SM-acceptors. The synthetic routes of the SM-acceptors are shown in Scheme 2, and the related syn- thesis methods and processes are summarized in Supporting Information (SI). In this study, from ITIC to POIT-IC, POIT- IC2F and then to POIT-IC4F, these SM-acceptors show gradually broadened absorption spectra, increased maximum extinction absorption coefficient, enhanced crystallinity, and electron mobi- lities due to the synergistic effects of side-chain engineering and fluorination. It is noted that POIT-IC2F and POIT-IC4F with fluorine on the end groups exhibit broader absorption spectra when compared with non-fluorinated ITIC and POIT-IC, and higher LUMO levels relative to the analogues with alkylphenyl as side chains such as IT-IC2F and IT-IC4F, which are conducive to higher open-circuit voltage (V_{oc}) for OSCs. As we expected, combined with fluorinated wide bandgap polymer donor PM6[30,51–53] as shown in Scheme 2, the annealing-free OSCs based on POIT-IC4F achieved a PCE of up to 13.8% with a high V_{oc} of 0.91 V, a low-energy loss (E_{loss}, is defined as E_g^{opt} eV_{oc}, where E_g^{opt} is optical bandgap of SM-acceptors in this work) of 0.58 eV, a J_{sc} of 20.9 mA cm ^{2}, and an FF of 72.6%, which is significantly higher than that of the ITIC (PCE 8.9%), POIT-IC (PCE 10.1%), or IT-IC4F (PCE 12.2%)-based control OSCs under the same processing conditions, and also is one of the highest PCEs reported for the annealing-free OSCs.

2. Result and Discussion

As shown in Figure 1a, in both chlorobenzene (CB) solutions and thin films, as the fluorination increases, the absorption onsets of the acceptors gradually red-shift due to the enhanced intramolecular electron push–pull effects. In films, compared with original ITIC (1.06 x 10^5 cm ^{1} at *ca*. 702 nm), POIT-IC

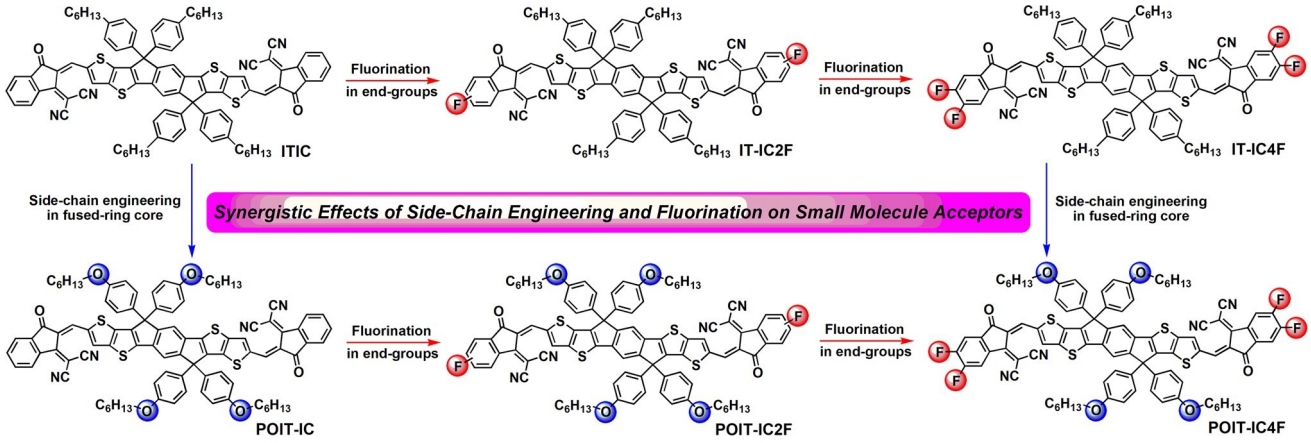

Scheme 1. A schematic diagram of the molecular structure optimization of ITIC derivatives: the blue arrow is side-chain engineering in fused-ring core and the red arrow is fluorination in end groups.

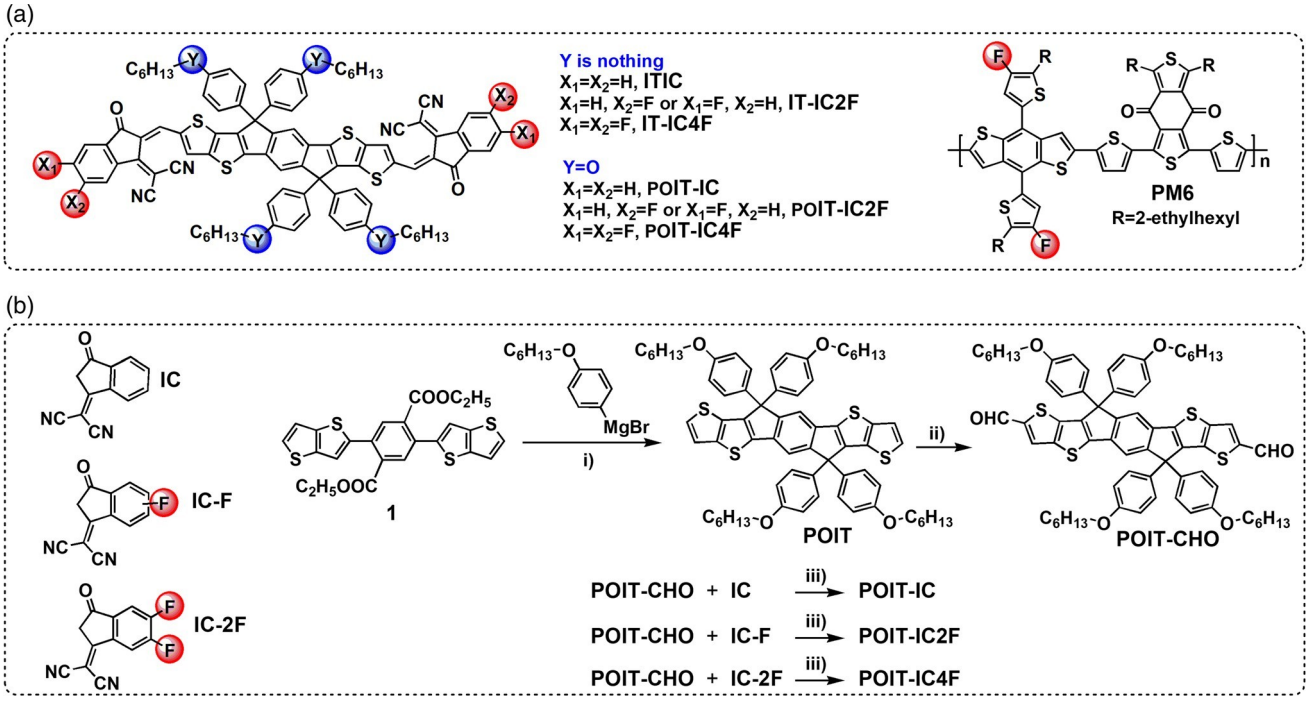

Scheme 2. a) The molecular structures of ITIC-type SM-acceptors and polymer donor PM6. b) The synthetic routes of new SM-acceptors POIT-IC, POIT-IC2F, and POIT-IC4F.

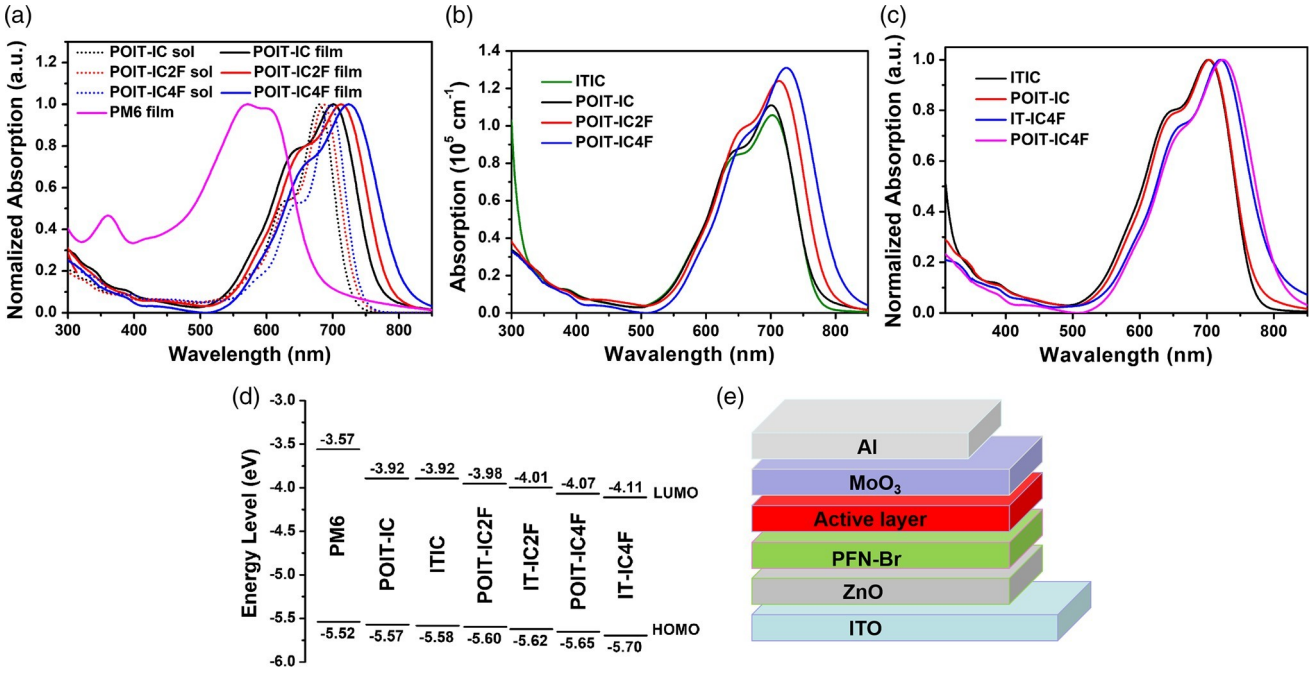

Figure 1. a) The normalized absorption spectra of the three new SM-acceptors in chlorobenzene solutions and in films, and polymer PM6 film. b) The absorption spectra of the three new SM-acceptors, as well as ITIC in films. c) The normalized absorption spectra of ITIC, POIT-IC, IT-IC4F, and POIT-IC4F.
d) The energy-level diagrams of the polymer donor and SM-acceptors. e) The device structure of OSCs.

with alkoxyphenyl side chains exhibits a slightly higher maxi- mum absorption coefficient (1.10 x 10^5 cm^{-1} at *ca*. 704 nm), while POIT-IC2F (1.24 x 10^5 cm^{-1} at *ca*. 716 nm) and POIT- IC4F (1.31 x 10^5 cm^{-1} at *ca*. 725 nm) display the significantly

red-shifted absorption peaks and increased maximum absorp- tion coefficient due to the synergistic effects of alkoxyphenyl side-chain engineering and fluorination on the SM-acceptors (see Figure 1b). Also the four SM-acceptors have progressively red-shifted absorption onsets at *ca*. 779, 784, 801, and 829 nm, corresponding to the optical bandgap (E_g^{opt} is defined as $1240/\lambda_{onset}$) of 1.59, 1.58, 1.55, and 1.49 eV, respectively. Moreover, comparing IT-IC4F with alkylphenyl side chains
(E_g^{opt} is ⬚.52 eV), POIT-IC4F film also exhibits red-shifted absorption spectrum (see Figure 1c). The higher absorption coefficient and red-shifted absorption spectra are conducive to
capture more photons for the related OSCs.

The cyclic voltammograms of the new SM-acceptors are shown in Figure S1, Supporting Information. The schematic diagrams of molecular energy levels of the polymer PM6 and six SM-acceptors are shown in Figure 1d. Furthermore, the SM-acceptors usually show lower molecular energy levels as fluorination increases in electron-accepting end groups. Interestingly, the fluorinated SM-acceptors with alkoxyphenyl side chains exhibit slightly higher LUMO levels than the fluorinated SM-acceptors with alkylphenyl side chains, although they have red-shifted absorption spectra, which will help the related OSCs achieve both higher V_{oc} and J_{sc}. Moreover, the electron mobilities (μ_e) of the new SM-acceptors also were measured using the space-charge-limited current (SCLC) method. As shown in Figure S2a, Supporting Information, the tetra-fluorinated POIT-IC4F has a higher μ_e of
4.22×10^{-4} cm^2 V^{-1} s^{-1} than those of difluorinated POIT-IC2F (2.18×10^{-4} cm^2 V^{-1} s^{-1}) and nonfluorinated POIT-IC (1.79×10^{-4} cm^2 V^{-1} s^{-1}).

The synergistic boosting effects of side-chain engineering and fluorination on the photovoltaic performance of the SM- acceptors were probed by fabricating the OSCs with an inverted device structure of ITO/ZnO/PFN-Br/active layer/MoO_3/Al. The optimized active layers of donor:acceptor (D:A, PM6:SM- acceptor) were gained by coating the blend solutions (volume ratio of CB:1,8-diiodooctane is 100:1) with a D:A weight ratio of 1:1 and a total concentration of 22 mg mL^{-1}. The current density–voltage (*J*–*V*) plots of OSCs are shown in Figure 2a, and the corresponding key device data are listed in Table 1. From the PM6:POIT-IC to the PM6:POIT-IC2F, and then to the PM6:POIT-IC4F-based OSCs, the devices show the gradually decreased V_{oc} from 1.04 to 0.91 V, an increased J_{sc} from 16.1 to
20.9 mA cm^{-2}, and an FF from 60.1% to 72.6%, which is consis-
tent with the variation trends of molecular LUMO levels, absorp- tion coefficient and range, as well as electron mobilities of the SM-acceptors. Ultimately, due to the efficient fluorination of POIT-IC4F, the PM6:POIT-IC4F-based OSCs achieved a high PCE of 13.8%, which is significantly higher than those of the OSCs based on POIT-IC (PCE 10.1%) or POIT-IC2F
(PCE¼ 12.4%). It is noted that about 13.8% efficiency is one of the highest PCEs recorded for annealing-free OSCs.

To better understand the effects of alkoxy side-chain engineer- ing on molecular photovoltaic performance, we also fabricated the ITIC-based and IT-IC4F-based OSCs under the same proc- essing conditions as a comparison. As shown in Figure 2c and Table 1, the ITIC-based and POIT-IC-based OSCs achieved almost the same V_{oc} of *ca*. 1.04 V, which means that alkoxy sub- stituents can slightly reduce the E_{loss} of related devices while

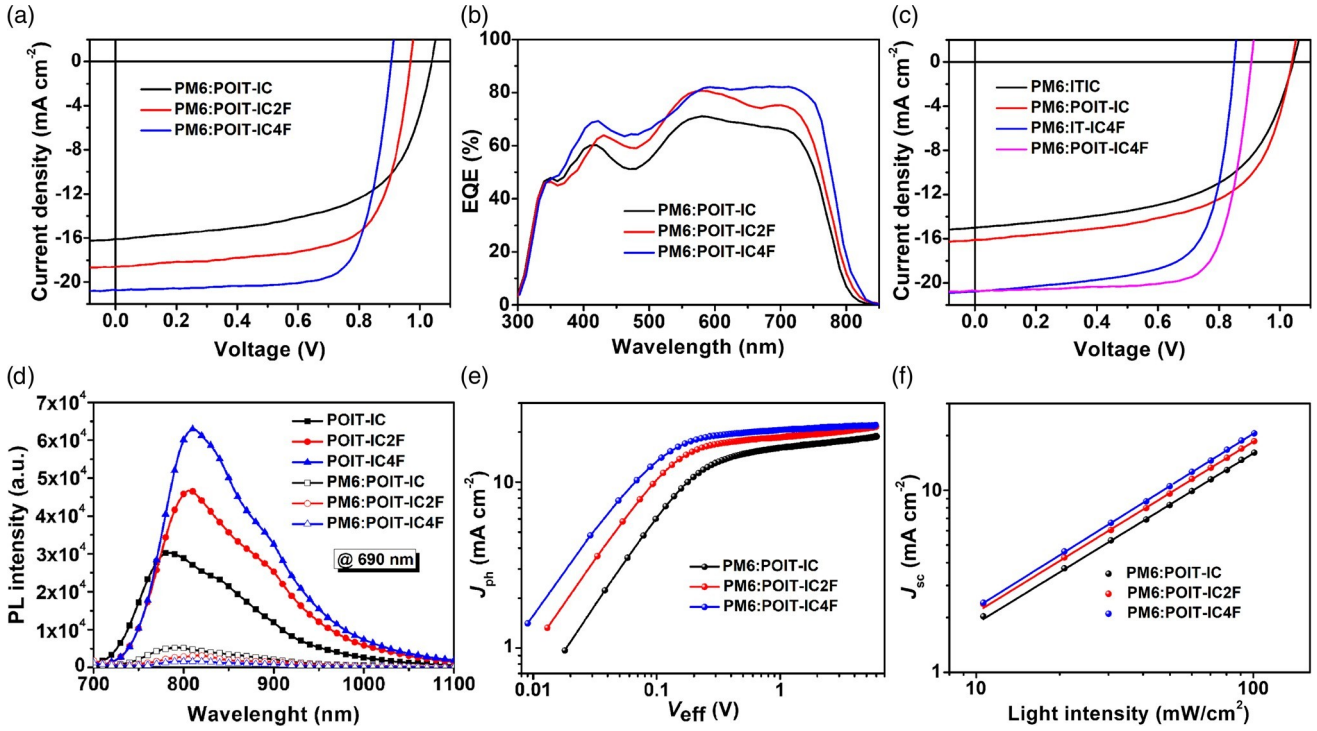

Figure 2. a) The *J*–*V* plots of the OSCs based on new SM-acceptors and b) the related EQE plots. c) The *J*-*V* plots of the OSCs based on different SM-acceptors of ITIC, POIT-IC, IT-IC4F, and POIT-IC4F. d) The PL spectra of new SM-acceptor pure films and the related blend films. e) The *J*ph versus *V*eff, and f) the *J*sc versus light intensity of the OSCs based on new SM-acceptors.

Table 1. Photovoltaic data of the annealing-free OSCs based on PM6:SM- acceptors.

Active layers	V_{oc} [V]	J_{sc} [mA cm^{-2}][a]	FF [%]	PCE [%][b]	E_{loss} [eV]
PM6:POIT-IC	1.04	16.1 (15.8)	60.1	10.1 (9.7)	0.54
PM6:POIT-IC2F	0.97	18.6 (17.9)	68.5	12.4 (11.9)	0.61
PM6:POIT-IC4F	0.91	20.9 (20.0)	72.6	13.8 (13.4)	0.58
PM6:ITIC	1.04	15.1	57.1	8.9 (8.5)	0.55

[a] The integral J_{sc} in parenthesis from the EQE curves. [b] The average PCEs in parenthesis calculated from 20 devices.

broadening the spectra in this study. Moreover, compared with the ITIC-based OSCs, the POIT-IC-based OSCs obtained higher J_{sc} and FF values due to the broadened absorption spectrum, increased absorption coefficient, and electron mobility of POIT-IC than ITIC. Similar phenomena have also been found in other OSCs. For instance, compared to the IT-IC4F film with an E_g^{opt} of 1.52 eV and the PM6:IT-IC4F-based OSCs with a V_{oc} of 0.85 V and an E_{loss} of 0.67 eV, the POIT-IC4F film showed a slightly lower E_g^{opt} of 1.49 eV and the related OSCs based on PM6:POIT-IC4F achieved a higher V_{oc} of 0.91 V and a lower E_{loss} of 0.58 eV. This is the first study that broadens the molecular absorption spectra of the SM-acceptors by a slightly changed side- chain engineering, while minimizing the voltage loss of the related OSCs. As a result, the PCE of the OSCs based on POIT-IC4F is increased by 15% when compared with that of the OSCs based on IT-IC4F.

The external quantum efficiency (EQE) tests were performed to understand the photon collection processes. As shown in Figure 2b, all of the OSCs based on the new SM-acceptors showed efficient EQE response values in the region of 650 820 nm belonging to the absorption range of SM-acceptors, which implies that ultrafast and efficient hole transfer happened from SM-acceptors to PM6 despite the HOMO offsets between them being only 0.05 0.13 eV.[19,51] From the PM6:POIT-IC to PM6:POIT-IC2F and then to PM6:POIT-IC4F-based devices, the OSCs showed gradually improved EQE values, especially in the absorption range of 650 820 nm belonging to the SM-acceptors, which is consistent with the changing trend of absorption coefficient of the SM-acceptors. The integrated J_{sc} from the EQE plots are 15.8, 17.9, and 20.0 mA cm^{-2} for the OSCs based on POIT-IC, POIT-IC2F, and POIT-IC4F, respectively, which agrees well with the J–V characteristics.

As shown in Figure 2d, the photoluminescence (PL) spectra of the new SM-acceptor pure films and related blend films with PM6 were probed. With the introduction of side-chain engineer- ing and fluorination, the SM-acceptor pure films displayed the gradually increased PL intensities under the excitation wavelength of 690 nm, which means that POIT-IC4F film has less thermal radiation loss under light. Moreover, compared to the PL spectra of pure films, the PM6:POIT-IC, PM6:POIT-IC2F, and PM6:POIT-IC4F blend films displayed the gradually increased PL quenching efficiencies of 83%, 93.4%, and 97.1%, respectively. These results imply that there is a more effi- cient exciton dissociation process between PM6 and POIT-IC4F, which is beneficial for higher Jsc in devices. The above results are consistent with the variation trends of J_{sc} and FF values in devices.

The exciton dissociation probability $P(E,T)$ can be used to eval- uate the exciton dissociation and the charge extraction capabili- ties of OSCs from the plots of photocurrent (J_{ph}) versus effective voltage (V_{eff}) (see Figure 2e and the section of devices character- zation in Supporting Information).[54,55] The PM6:POIT- IC-based, PM6:POIT-IC2F-based, and PM6:POIT-IC4F-based devices exhibited a gradual increase in $P(E,T)$ values i.e., 74.2%, 82.8%, and 85.1% under the maximal power output

conditions, respectively, which imply that the OSCs based on tetra-fluorinated POIT-IC4F have more efficient exciton dissoci- ation and charge extraction processes. Moreover, as shown in Figure 2f, the effect of light intensity (P) on J_{sc} was studied to probe the charge recombination properties of the OSCs. Usually, the relationship of P and J_{sc} is defined as $J_{sc} \propto P^S$, where the S value is close to 1 if the OSCs have weak bimolecular recombination.[54,56] With the enhancement of fluorination on the SM-acceptors, the PM6-based OSCs achieved the S values approaching 1 gradually from 0.93 to 0.94, and then to 0.96, respectively, suggesting that the fluorination of SM-acceptors can efficiently decrease the bimolecular recombination of OSCs in this case. Moreover, from PM6:POIT-IC to PM6: POIT-IC2F and then to PM6:POIT-IC4F, the blend films dis- played a gradual increase and more balanced electron/hole mobi- lities (μ_e/μ_h) from 6.44/0.35 10^{-4} to 6.57/1.59 10^{-4} and then to 8.02/2.09 10^{-4} cm^2 V^{-1} s^{-1} in the mobility measurements using the SCLC method, as shown in Figure S2a, Supporting Information. Usually, the high and balanced μ_e/μ_h of the D/A blend films can suppress space charge accumulation and improve charge extraction, and thereby facilitate to achieve a high J_{sc} and FF, which are consistent with the device performances. The molecular crystallinity and packing of PM6, POIT-IC, POIT-IC2F, and POIT-IC2F pure films and the related blend films were studied by performing the grazing incidence wide- angle X-ray scattering (GIWAXS) measurements.[57] The 2D GIWAXS diffraction images are shown in Figure 3a, and the related out-of-plane (OOP) and in-plane (IP) line cuts from 1D profiles are shown in Figure 3b,c, respectively. In pure films, all three SM-acceptors show a mixed orientation that includes “edge-on” and “face-on” orientations. In IP direction, comparing POIT-IC film with a (100) diffraction peak at 0.334 $Å^{-1}$, a crys- tal coherence length (CCL) of 2.28 nm, and a lamellar distance of 18.8 Å, POIT-IC2F film shows a higher CL of 2.33 nm and a smaller lamellar distance of 18.2 Å at 0.344 $Å^{-1}$. When com- pared with POIT-IC2F, POIT-IC4F achieves the stronger fluori- nation with a higher CCL of 2.39 nm and a smaller lamellar distance of 17.9 Å at 0.344 $Å^{-1}$, which implies that the fluori- nation can improve the crystalline quality of the SM-acceptors. In OOP direction, POIT-IC4F film has a smaller π–π stacking dis- tance of 4.09 Å when compared with POIT-IC2F film with a π–π stacking distance of 4.11 Å and POIT-IC film with a π–π stacking distance of 4.15 Å. The stronger crystallinity, smaller lamellar, and π–π stacking distances are conducive to gain higher electron mobility in POIT-IC4F film (Figure S2, Supporting Information). All the blend films show a predominant “face-on” orientation, arising from the regular arrangement of polymer molecules. Furthermore, with the introduction of fluorination on the

× × □ □ □

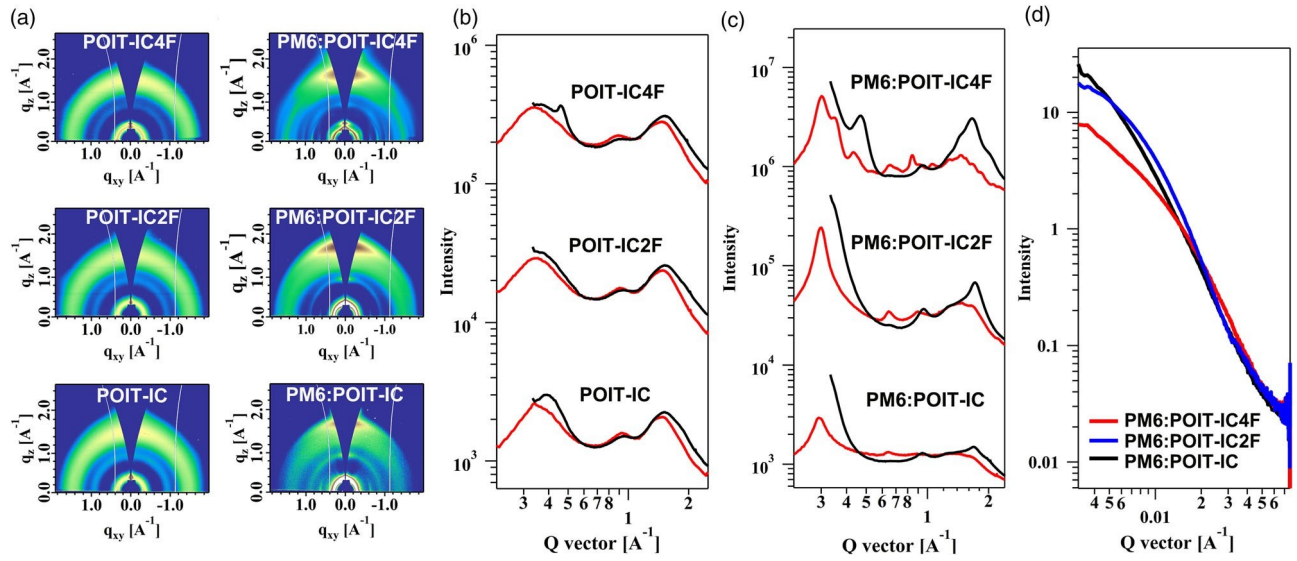

Figure 3. a) The 2D GIWAXS profiles, and the related IP (red) and OOP (black) line-cuts in the 1D GIWAXS profiles of b) the SM-acceptor pure films and
c) the related blend films. d) The RSoXS profiles of the blend films.

SM-acceptors, the related blend films display the gradually increased intermolecular π–π stacking as evidenced by stronger and sharper π–π stacking in OOP directions. It can be observed that PM6:POIT-IC4F blend shows the closest π–π stacking, indi- cating an enhanced molecular interaction, which is beneficial for electron hopping. To achieve the optimum blend film

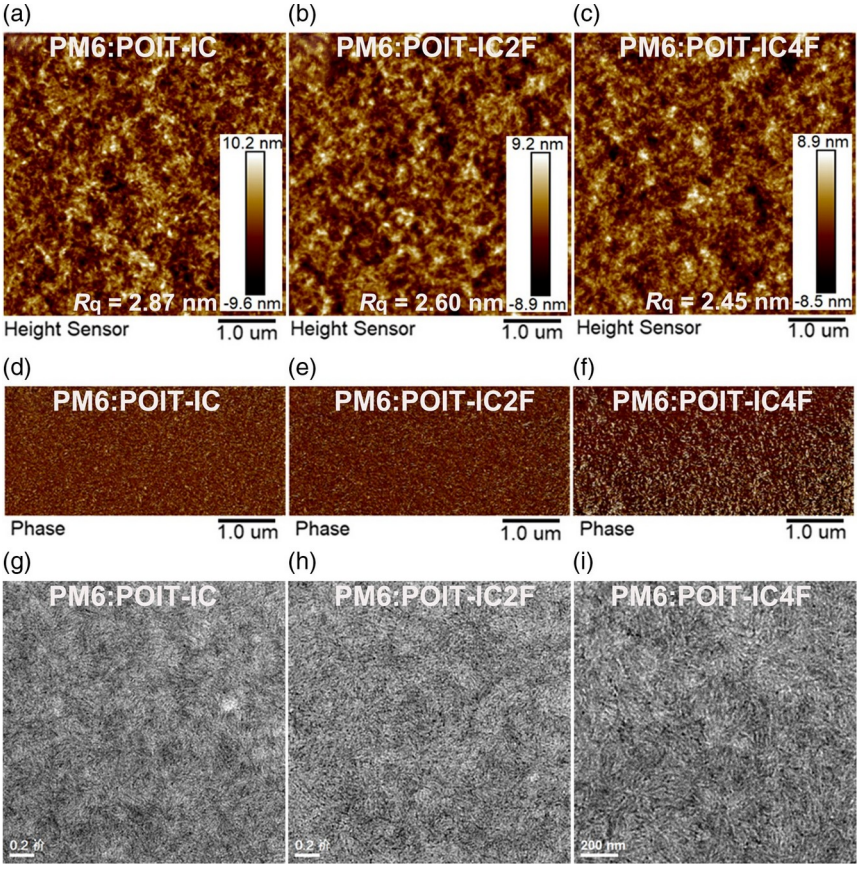

Figure 4. The AFM (a–c are height images and d–f are phase images) and TEM g–i) images of the blend films: a,d,g) for PM6:POIT-IC film; b,e,h) for PM6:POIT-IC2F film; and c,f,i) for PM6:POIT-IC4F film, respectively.

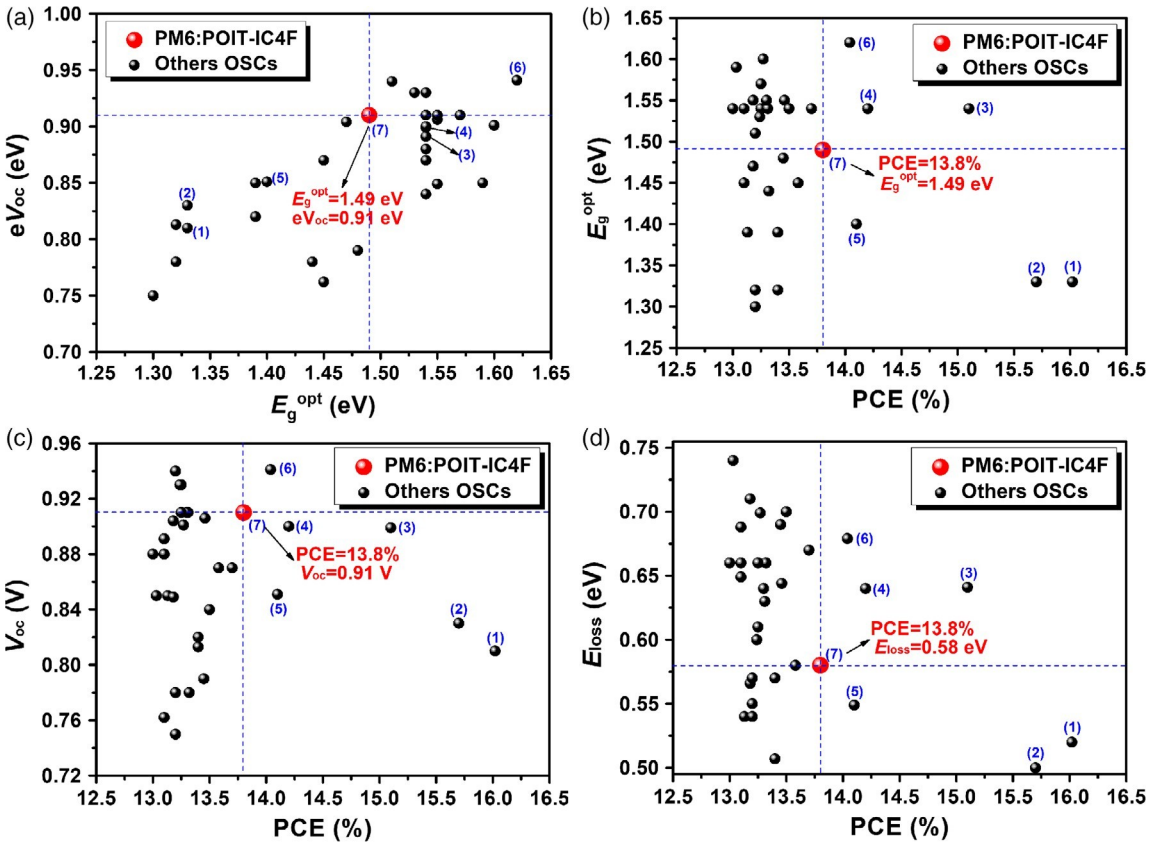

Figure 5. a) Plots of eV_{oc} versus E_g^{opt}, as well as b) E_g^{opt} c) V_{oc} and d) E_{loss} versus PCE in the various single-junction OSCs based on the binary active layer (PCE > 13%).

morphology, an effective strategy is to maintain good crystallinity of both the PM6 and SM-acceptor components within a proper phase-separated network in active layers.[9c] Here, the PM6: POIT-IC and PM6:POIT-IC2F films have the very weak SM-acceptor peaks in OOP direction, which means that the crys- tallization of SM-acceptors is depressed, arising from its good miscibility with polymer PM6. Conversely, the PM6:POIT- IC4F blend film shows an obvious (010) diffraction peak at
1.46 Å ^{1} belonging to POIT-IC4F, indicating that the introduc- tion of four fluorine atoms significantly changes the intermolec- ular interaction between polymer donor and SM-acceptor. The face-on orientation, an improved π–π stacking, and the crystallin- ity of POIT-IC4F in blend are conducive to reduce the probability of trap-assisted recombination and obtain a more efficient charge transfer in OSCs, and thus achieve higher J_{sc} and FF.

The length scale of phase separation of BHJ blends is charac-
terized using resonant soft X-ray scattering (RSoXS), and the results are shown in Figure 3d. It is seen that PM6:POIT-IC blend shows a quite quick decay in intensity, and not much structure could be observed. Thus, PM6 and POIT-IC can form a quite good mixture in blends, which reduces the FF and PCE in OSCs. When compared with PM6:POIT-IC2F blend, the PM6:POIT-IC4F blend shows a new scattering shoulder at 0.022 Å ^{1}, corresponding to a centre-to-centre distance of 28.5 nm, which is the length scale between the fibers. Such a blend morphology with suitable scale of

phase separation and fibril-like interpenetrating network structure is beneficial for exciton dissociation and charge transport, and thus an improved *FF* and J_{sc} is available.

The surface morphologies of active layers were investigated using atomic force microscopy (AFM) measurements, as shown in Figure 4a–c. In the AFM height images, all the active layers display smooth surface morphologies with the small and similar root-mean-square roughness (R_q) of 2.45 2.87 nm, which means that the fluorination of SM-acceptors does not significantly affect the surface roughness of the related active layers. In AFM phase images (Figure 4d–f), with an increase in fluorination on the SM- acceptors, the corresponding active layers show the gradually improved phase separation with uniform fibril texture. The similar phenomenon of improving phase separation of active layers was also observed in transmission electron microscopy (TEM) images. As shown in Figure 4g–i, the active layers have a gradual phase separation from PM6:POIT-IC to PM6:POIT-IC2F and then to PM6:POIT-IC4F. Also the PM6:POIT-IC4F blend film displays more regular bicontinuous interpenetrating network structure and fibril texture with an appropriate size of 20 nm, which is conducive to exciton separation and charge transport, and thus improving the J_{sc} and FF values of the related OSCs.

The correlations of eV_{oc} versus E_g^{opt}, as well as E^{opt}, V_{oc}, and E_{loss} versus PCE in this study (PM6:POIT-IC4F) compared with the other efficient single-junction OSCs based on the binary

~

g

active layer (PCE > 13%) are shown in Figure 5 and Table S1, Supporting Information. In the reported literatures, the E_{loss} of OSCs is mainly concentrated in 0.65 – 0.80 eV, which is higher than the empirical limit value of 0.60 eV. Only a few of the OSCs based on active layer materials with the wide absorption spectra and matched energy levels have been reported to maximize the V_{oc} value and minimize the E_{loss} value simultaneously. In this study, we fabricated the PM6:POIT-IC4F-based OSCs that can achieve high photovoltage under small voltage loss. Because of the small E_g^{opt} (1.49 eV) in the POIT-IC4F film and the high V_{oc} (0.91 V) in the PM6:POIT-IC4F-based OSCs, the devices achieve a small E_{loss} of 0.58 eV, which is lower than the empirical limit value of 0.60 eV. However, it is very difficult to achieve high PCEs at low E_{loss} in OSCs because of the inherent trade-off between V_{oc} and J_{sc}. Here, if the E_{loss} is lower than the empir-ical limit of 0.6 eV, the OSCs still obtain high PCE of 13.8% (Figure 5d), which is due to the related active layer that has high absorption coefficient, good morphology, as well as the small ΔE_{HOMO} of 0.13 eV between PM6 and POIT-IC4F.[19,31,40] It is noted that the PCE of 13.8% is one of the highest values in the reported literatures for the OSCs with a V_{oc} of over 0.90 V (Figure 5c), and for the OSCs with a E_{loss} lower than 0.60 eV (Figure 5d).

3. Conclusions

In conclusion, three new SM-acceptors, POIT-IC, POIT-IC2F, and POIT-IC4F, were developed by combining the alkoxy side- chain engineering and fluorination. From ITIC to POIT-IC, POIT-IC2F, and then to POIT-IC4F, these SM-acceptors show improved absorption spectrum and coefficient, as well as enhanced crystallinity and electron mobilities. When compared with nonfluorinated ITIC and POIT-IC, as the introduction of fluorine to broaden the molecular absorption spectra, POIT-IC2F and POIT-IC4F with alkoxyphenyl side chains show less decreased LUMO levels than IT-IC2F and IT-IC4F with alkyl- phenyl side chains, which are conducive to both V_{oc} and J_{sc} for OSCs. As we expected, combined with fluorinated polymer donor PM6, the annealing-free OSCs based on POIT-IC4F achieved a high PCE of 13.8% with a high V_{oc} of 0.91 V, a low E_{loss} of 0.58 eV, a J_{sc} of 20.9 mA cm^{-2}, and a FF of 72.6%, which is higher than those of the control OSCs based on ITIC (PCE 8.9%), POIT-IC (PCE 10.1%), or IT-IC4F (PCE 12.2%) under the same processing conditions, and also is one of the highest PCEs reported for the annealing-free OSCs with a V_{oc} of over 0.90 V and a E_{loss} lower than 0.60 eV.

Acknowledgements

the U.S. Office of Naval Research under contract N00014-15-1-2244. Portions of this research were carried out at beamline 7.3.3 and 11.0.1.2 at the Advanced Light Source, Molecular Foundry, and National Center for Electron Microscopy, Lawrence Berkeley National Laboratory, which was supported by the DOE, Office of Science, and Office of Basic Energy Sciences.

Conflict of Interest

The authors declare no conflict of interest.

Keywords

fluorination, organic solar cells, power conversion efficiency, side-chain engineering, small molecule acceptors

[1] a) Y. Li, *Acc. Chem. Res.* 2012, *45*, 723; b) Q. Fan, W. Su, X. Guo, B. Guo, W. Li, Y. Zhang, K. Wang, M. Zhang, Y. Li, *Adv. Energy Mater.* 2016, *6*, 1600430.

[2] J. Zhao, Y. Li, G. Yang, K. Jiang, H. Ade, W. Ma, H. Yan, *Nat. Energy* 2016, *1*, 15027.

[3] H. Chen, Z. Hu, L. Liu, P. Chao, J. Qu, W. Chen, A. Liu, F. He, *Joule* 2018, *2*, 1623.

[4] D. Deng, Y. Zhang, J. Zhang, Z. Wang, L. Zhu, B. Xia, Z. Wang, K. Lu, W. Ma, Z. Wei, *Nat. Commun.* 2016, *7*, 13740.

[5] a) R. Sun, J. Guo, T. Wang, Z. Luo, Z. Zhang, X. Jiao, W. Tang, C. Yang, Y. Li, J. Min, *Energy Environ. Sci.* 2019, *12*, 384; b) Q. An, J. Wang, F. Zhang, *Nano Energy* 2019, *60*, 768.

[6] a) K. Gao, S. B. Jo, X. Shi, L. Nian, M. Zhang, Y. Kan, F. Lin, B. Xu, Q. Rong, L. Shui, F. Liu, X. Peng, G. Zhou, Y. Cao, A. K.-Y. Jen, *Adv. Mater.* 2019, *31*, 1807842; b) W. Su, Q. Fan, X. Guo, X. Meng, Z. Bi, W. Ma, M. Zhang, Y. Li, *Nano Energy* 2017, *38*, 510.

[7] X. Du, T. Heumueller, W. Gruber, A. Classen, T. Unruh, N. Li, C. J. Brabec, *Joule* 2019, *3*, 215.

[8] Y. Zhou, M. Li, J. Song, Y. Liu, J. Zhang, L. Yang, Z. Zhang, Z. Bo, H. Wang, *Nano Energy* 2018, *45*, 10.

[9] a) B. Xiao, A. Tang, J. Zhang, Z. Wei, E. Zhou, *Adv. Energy Mater.* 2017, *7*, 1602269; b) Q. Fan, T. Liu, W. Gao, Y. Xiao, J. Wu, W. Su, X. Guo, X. Lu, C. Yang, H. Yan, M. Zhang, Y. Li, *J. Mater. Chem. A* 2019, *7*, 15404. c) Q. Fan, Z. Xu, X. Guo, X. Meng, W. Li, X. Ou, W. Ma,

M. Zhang, Y. Li, *Nano Energy* 2017, *40*, 20.
[10] G. Gao, N. Liang, H. Geng, W. Jiang, J. Feng, J. Hou, X. Feng, Z. Wang, *J. Am. Chem. Soc.* 2017, *139*, 15914.
[11] a) D. Baran, R. Ashraf, D. Hanifi, M. Abdelsamie, N. Gasparini, J. Röhr, S. Holliday, M. Neophytou, J. Nelson, C. Brabec, A. Amassian, A. Salleo, T. Kirchartz, J. Durrant, I. McCulloch, *Nat. Mater.* 2017, *16*, 363; b) Q. Fan, W. Su, X. Meng, X. Guo, G. Li, W. Ma, M. Zhang, Y. Li, *Sol. RRL* 2017, *1*, 1700020.
[12] G. Feng, J. Li, F. J. Colberts, M. Li, J. Zhang, F. Yang, Y. Jin, F. Zhang, R. Janssen, C. Li, W. Li, *J. Am. Chem. Soc.* 2017, *139*, 18647.
[13] a) Z. Yao, X. Liao, K. Gao, F. Lin, X. Xu, X. Shi, L. Zuo, F. Liu, Y. Chen, A. K.-Y. Jen, *J. Am. Chem. Soc.* 2018, *140*, 2054; b) Q. Fan, W. Su, X. Guo, Y. Wang, J. Chen, C. Ye, M. Zhang, Y. Li, *J. Mater. Chem. A* 2017, *5*, 9204; c) Q. An, W. Gao, F. Zhang, J. Wang, M. Zhang, K. Wu, X. Ma, Z. Hu, C. Jiao, C. Yang, *J. Mater. Chem. A* 2018, *6*, 2468.
[14] Y. Hwang, H. Li, B. Courtright, S. Subramaniyan, S. Jenekhe, *Adv. Mater.* 2016, *28*, 124.

Q.F., W.S., and M.Z. contributed equally to this work. This work was sup-ported by National Natural Science Foundation of China (NSFC) (Nos. 51573120, 51773142, and 91633301), Collaborative Innovation Center of Suzhou Nano Science and Technology. T. P. Russell was supported by

[15] Y. Li, J. Lin, X. Che, Y. Qu, F. Liu, L. Liao, S. Forrest, *J. Am. Chem. Soc.* 2017, *139*, 17114.
[16] C. Li, J. Song, L. Ye, C. Koh, K. Weng, H. Fu, Y. Cai, Y. Xie, D. Wei, H. Woo, Y. Sun, *Sol. RRL* 2019, *3*, 1800246.
[17] R. Lv, D. Chen, X. Liao, L. Chen, Y. Chen, *Adv. Funct. Mater.* 2019, *29*, 1805872.
[18] a) Z. Xiao, S. Yang, Z. Yang, J. Yang, H. Yip, F. Zhang, F. He, T. Wang, J. Wang, Y. Yuan, H. Yang, M. Wang, L. Ding, *Adv. Mater.* 2018, *30*, 1804790; b) Q. An, F. Zhang, W. Gao, Q. Sun, M. Zhang, C. Yang, J. Zhang, *Nano Energy* 2018, *45*, 177; c) W. Su, Q. Fan, X. Guo, B. Guo, W. Li, Y. Zhang, M. Zhang, Y. Li, *J. Mater. Chem. A* 2016, *4*, 14752.
[19] S. Li, L. Zhan, H. Zhu, G. Zhou, W. Yang, M. Shi, C. Li, J. Hou, Y. Li, H. Chen, *J. Am. Chem. Soc.* 2019, *141*, 3073.
[20] T. Lee, Y. Eom, C. Song, I. Jung, D. Kim, S. Lee, W. Shin, E. Lim, *Adv. Energy Mater.* 2019, *9*, 1804021.
[21] Y. Lin, J. Wang, Z. Zhang, H. Bai, Y. Li, D. Zhu, X. Zhan, *Adv. Mater.* 2015, *27*, 1170.
[22] Y. Yang, Z. Zhang, H. Bin, S. Chen, L. Xue, C. Yang, Y. Li, *J. Am. Chem. Soc.* 2016, *138*, 15011.
[23] W. Zhao, H. Yao, S. Zhang, Y. Zhang, B. Yang, J. Hou, *J. Am. Chem. Soc.* 2017, *139*, 7148.
[24] J. Yuan, Y. Zhang, L. Zhou, G. Zhang, H. Yip, T. Lau, X. Lu, C. Zhu, H. Peng, P. A. Johnson, M. Leclerc, Y. Cao, J. Ulanski, Y. Li, Y. Zou, *Joule* 2019, *3*, 1140.
[25] B. Fan, D. Zhang, M. Li, W. Zhong, Z. Zeng, L. Ying, F. Huang, Y. Cao, *Sci. China Chem.* 2019, *62*, 746.
[26] a) Y. Cui, H. Yao, L. Hong, T. Zhang, Y. Xu, K. Xian, B. Gao, J. Qin, J. Zhang, Z. Wei, J. Hou, *Adv. Mater.* 2019, *31*, 1808356; b) X. Ma, M. Luo, W. Gao, J. Yuan, Q. An, M. Zhang, Z. Hu, J. Gao, J. Wang, Y. Zou, C. Yang, F. Zhang, *J. Mater. Chem. A* 2019, *7*, 7843; c) T. Liu, Z. Luo, Q. Fan, G. Zhang, L. Zhang, W. Gao, X. Guo, W. Ma, M. Zhang, C. Yang, Y. Li, H. Yan, *Energy Environ. Sci.* 2018, *11*, 3275.
[27] Y. Li, N. Zheng, L. Yu, S. Wen, C. Gao, M. Sun, R. Yang, *Adv. Mater.* 2019, *31*, 1807832.
[28] a) K. Feng, J. Yuan, Z. Bi, W. Ma, X. Xu, G. Zhang, Q. Peng, *iScience* 2019, *12*, 1; b) J. Chen, G. Li, Q. Zhu, X. Guo, Q. Fan, W. Ma, M. Zhang, *J. Mater. Chem. A* 2019, *7*, 3745.
[29] S. Li, L. Ye, W. Zhao, H. Yan, B. Yang, D. Liu, W. Li, H. Ade, J. Hou, *J. Am. Chem. Soc.* 2018, *140*, 7159.
[30] Q. Fan, W. Su, Y. Jiang, X. Guo, F. Liu, T. P. Russell, M. Zhang, Y. Li, *Sci. China Chem.* 2018, *61*, 531.
[31] X. Li, F. Pan, M. Zhang, Z. Wang, J. Du, J. Wang, M. Xiao, L. Xue, Z. Zhang, C. Zhang, F. Liu, Y. Li, *Nat. Commun.* 2019, *10*, 519.
[32] W. Liu, J. Zhang, Z. Zhou, D. Zhang, Y. Zhang, S. Xu, X. Zhu, *Adv. Mater.* 2018, *30*, 1800403.
[33] a) R. Geng, X. Song, H. Feng, J. Yu, M. Zhang, N. Gasparini, Z. Zhang, F. Liu, D. Baran, W. Tang, *ACS Energy Lett.* 2019, *4*, 763; b) M. Zhang, Z. Xiao, W. Gao, Q. Liu, K. Jin, W. Wang, Y. Mi, Q. An, X. Ma, X. Liu, C. Yang, L. Ding, F. Zhang, *Adv. Energy Mater.* 2018, *8*, 1801968.
[34] J. Yu, P. Chen, C. Koh, H. Wang, K. Yang, X. Zhou, B. Liu, Q. Liao, J. Chen, H. Sun, H. Woo, S. Zhang, X. Guo, *Adv. Sci.* 2019, *6*, 1801743.

[35] W. Wang, B. Zhao, Y. Xie, H. Wu, Q. Liang, S. Liu, F. Liu, C. Gao, H. Wu, Y. Cao, *ACS Energy Lett.* 2018, *3*, 1499.
[36] W. Gao, T. Liu, R. Ming, K. Wu, L. Zhang, J. Xin, D. Xie, G. Zhang, W. Ma, H. Yan, C. Yang, *Adv. Funct. Mater.* 2018, *28*, 1803128.
[37] J. Wang, K. Liu, L. Hong, G. Ge, C. Zhang, J. Hou, *ACS Energy Lett.* 2018, *3*, 2967.
[38] J. Zhu, Y. Xiao, J. Wang, K. Liu, H. Jiang, Y. Lin, X. Lu, X. Zhan, *Chem. Mater.* 2018, *30*, 4150.
[39] a) H. Feng, Y. Yi, X. Ke, J. Yan, Y. Zhang, X. Wan, C. Li, N. Zheng, Z. Xie, Y. Chen, *Adv. Energy Mater.* 2019, *9*, 1803541; b) W. Su, Q. Fan, X. Guo, J. Chen, Y. Wang, X. Wang, P. Dai, C. Ye, X. Bao, W. Ma, M. Zhang, Y. Li, *J. Mater. Chem. A* 2018, *6*, 7988.
[40] J. Hou, O. Inganäs, R. H. Friend, F. Gao, *Nat. Mater.* 2018, *17*, 119.
[41] Z. Liang, M. Li, X. Zhang, Q. Wang, Y. Jiang, H. Tian, Y. Geng, *J. Mater. Chem. A* 2018, *6*, 8059.
[42] a) D. He, F. Zhao, J. Xin, J. Rech, Z. Wei, W. Ma, W. You, B. Li, L. Jiang, Y. Li, C. Wang, *Adv. Energy Mater.* 2018, *8*, 1802050; b) W. Su, G. Li, Q. Fan, Q. Zhu, X. Guo, J. Chen, J. Wu, W. Ma, M. Zhang, Y. Li, *J. Mater. Chem. A* 2019, *7*, 2351.
[43] Y. Lin, T. Li, F. Zhao, L. Han, Z. Wang, Y. Wu, Q. He, J. Wang, L. Huo, Y. Sun, C. Wang, W. Ma, X. Zhan, *Adv. Energy Mater.* 2016, *6*, 1600854.
[44] J. Qu, Q. Zhao, J. Zhou, H. Lai, T. Liu, D. Li, W. Chen, Z. Xie, F. He, *Chem. Mater.* 2019, *31*, 1664.
[45] C. Yan, S. Barlow, Z. Wang, H. Yan, A. Jen, S. Marder. X. Zhan, *Nat. Rev. Mater.* 2018, *3*, 18003.
[46] G. Liu, J. Jia, K. Zhang, X. Jia, Q. Yin, W. Zhong, L. Li, F. Huang, Y. Cao, *Adv. Energy Mater.* 2019, *9*, 1803657.
[47] S. Feng, C. Zhang, Y. Liu, Z. Bi, Z. Zhang, X. Xu, W. Ma, Z. Bo, *Adv. Mater.* 2017, *29*, 1703527.
[48] Y. Lin, F. Zhao, Q. He, L. Huo, Y. Wu, T. Parker, W. Ma, Y. Sun, C. Wang, D. Zhu, A. Heeger, S. Marder, X. Zhan, *J. Am. Chem. Soc.* 2016, *138*, 4955.
[49] Z. Fei, F. Eisner, X. Jiao, M. Azzouzi, Y. Han, M. Shahid, A. Chesman, C. Easton, C. McNeill, T. Anthopoulos, J. Nelson, M. Heeney, *Adv. Mater.* 2018, *30*, 1705209.
[50] T. Aldrich, M. Matta, W. Zhu, S. Swick, C. Stern, G. Schatz, A. Facchetti, F. Melkonyan, T. Marks, *J. Am. Chem. Soc.* 2019, *141*, 3274.
[51] M. Zhang, X. Guo, W. Ma, H. Ade, J. Hou, *Adv. Mater.* 2015, *27*, 4655.
[52] Y. Wang, Q. Fan, X. Guo, M. Zhang, *J. Mater. Chem. A* 2017, *5*, 22180.
[53] Q. Fan, Y. Wang, M. Zhang, B. Wu, X. Guo, Y. Jiang, F. Liu, Z. Wei, T. Sum, T. Russell, Y. Li, *Adv. Mater.* 2018, *30*, 1704546.
[54] P. Blom, V. Mihailetchi, L. Koster, D. Markov, *Adv. Mater.* 2007, *19*, 1551.
[55] Q. Fan, Q. Zhu, X. Guo, W. Ma, M. Zhang, Y. Li, *Nano Energy* 2018, *48*, 413.
[56] M. Zhang, R. Ming, X. Ma, Z. Hu, C. Yang, F. Zhang, *Nano Energy* 2019, *59*, 58.
[57] a) W. Su, Y. Meng, X. Guo, Q. Fan, M. Zhang, Y. Jiang, Z. Xu, Y. Dai, B. Xie, F. Liu, M. Zhang, T. P. Russell, Y. Li, *J. Mater. Chem. A* 2018, *6*, 16403; b) L. Zhang, X. Xu, B. Lin, H. Zhao, T. Li, J. Xin, G. Qiu, S. Guo, K. Zhou, X. Zhan, W. Ma, *Adv. Mater.* 2018, *30*, 1805041.